# Default Network and Intelligence Difference

Ming Song, *Member, IEEE*, Yong Liu, Yuan Zhou, Kun Wang, Chunshui Yu, and Tianzi Jiang, *Senior Member, IEEE*

***Abstract*—In the last few years, many studies in the cognitive and system neuroscience found that a consistent network of brain regions, referred to as the default network, showed high levels of activity when no explicit task was performed. Some scientists believed that the resting state activity might reflect some neural functions that consolidate the past, stabilize brain ensembles, and prepare us for the future. Here, we modeled the default network as undirected weighted graph, and then used graph theory to investigate the topological properties of the default network of the two groups of people with different intelligence levels. We found that, in both groups, the posterior cingulate cortex showed the greatest degree in comparison to the other brain regions in the default network, and that the medial temporal lobes and cerebellar tonsils were topologically separations from the other brain regions in the default network. More importantly, we found that the strength of some functional connectivities and the global efficiency of the default network were significantly different between the superior intelligence group and the average intelligence group, which indicates that the functional integration of the default network might be related to the individual intelligent performance.**

***Index Terms*—Default network, functional magnetic resonance imaging (fMRI), intelligence, intrinsic activity.**

## I. Introduction

SCIENTISTS and engineers have been attempting to simulate human cognitive mechanisms to make an artificial intelligent system that exhibits mental capabilities, including perception, action, and motivation. One has been concerned primarily with the processes of how information is extracted from sensory inputs in an artificial system and integrated over time to make decisions and then take actions. So researchers have paid much attention to the dynamics when the system is required to make response to and interact with the external environment. Unfortunately, it seems that the progress is not exciting enough. An interesting question is what the artificial system does when it is idle. In other words, is it necessary to explore the significance of investigating the dynamics of the artificial system when the system is not explicitly engaged in the interaction with the external environment?

Manuscript received December 30, 2008; revised June 17, 2009. First published date August 04, 2009. Current version published October 21, 2009. This work was supported by the Natural Science Foundation of China, Grant 30730035, the National Key Basic Research and Development Program, Grant 2007CB512300, and the Excellent SKL Project of NSFC Grant 60723005.

M. Song, Y. Liu, Y. Zhou, K. Wang, and T. Jiang are with the Research Center of Computational Medicine, Sino-French Laboratory in Computer Science, Automation, and Applied Mathematics, Institution of Automation, Chinese Academy of Sciences, 100190 Beijing, P. R. China (e-mail: jiangtz@nlpr.ia.ac.cn).

C. S. Yu is with the Department of Radiology, Xuanwu Hospital of Capital Medical University, Beijing, P. R. China.

Color versions of one or more of the figures in this paper are available online at http://ieeexplore.ieee.org.

Digital Object Identifier 10.1109/TAMD.2009.2029312

On the other hand, some scientists in the cognitive and system neuroscience found that a consistent network of human brain regions showed high levels of activity when no explicit task was performed. They suggested that the human brain has a default or intrinsic mode of functioning [1]–[3]. As we know, the adult human brain represents about 2% of the body weight, yet requires about 20% of the body's total energy consumption. It is estimated that 60% to 80% of the brain's total energy consumption is used to maintain the neurons and their supporting cells. Surprisingly, the energy consumption associated with the evoked activity may account for only 0.5% to 1.0% of the brain's total energy consumption [2], [4]. Then what is the other brain's energy consumption used for? Although the unidentified part of brain's energy consumption is extremely larger than the task-evoked consumption, its physiological significance is not very clear. So some scientists called it as "dark energy" in the term of astronomic and believed that the "dark energy" is related to the brain's intrinsic activity, including the present in the so-called default network [4]. The default network is comprised of a set of brain regions, including medial prefrontal cortex, posterior midbrain regions, medial temporal lobes, lateral parietal cortex, and so on. These brain regions show greater neural activity during passive states in comparison to a range of cognitive task states. Although there are some arguments about cognitive functions of the default network [5]–[7], some investigators suggest that the brain's default network directly contributes to internal mentation that is largely detached from the external world, including self-reflective thoughts and judgments, conceiving the mental states of other peoples, and envisioning the future to make up alternative decisions [3]. Additionally, researchers have found the damaged activity of the default network in some neuropsychiatric diseases, for example, Alzheimer disease [8], schizophrenia [9], and in the coma and even vegetative state [10]. Taken together, these findings suggested that the intrinsic activity of the default network could play an important role in human cognitive functions.

For a long time, researchers have been concerned with some explicitly intelligence demanding tasks, for example, rational planning, reasoning, and working memory in order to understand the neural basis of the individual intelligence differences [11], [12]. In comparison, there are a few studies to investigate the associations between the intrinsic activity and the intelligent performance [13]–[18]. However, human brains are not only adaptive, but also anticipatory and prospective [19], [20]. Some scientists thought that it was the ability to reflect on the past and contemplate the future that facilitated the development of some unique human attributes, including imagination and creativity [4], [21], [22]. As mentioned above, the default network should support the neural activity for consolidating the past, stabilizing the brain's integration, and predicting the future [3], [6]. So it

is necessary to pay attention to the association between the different intelligent performance and the internal modes of cognition, especially, the activity of the default network.

In the present study, we explored the associations between the different human intelligent performance and the activity of the default network when the subjects were not required to do any explicitly cognitive tasks. Using the graph theory, we modeled the default network as undirected weighted graph for each subject and then investigated the network topology of the default network of the subjects.

## II. Materials and Methods

In the present study, we used the dataset that has been described previously to carry out the present study. For more details about the dataset and the data preprocessing, please refer to [17].

### A. Subjects

Fifty-nine healthy right-handed subjects were included in this study. The Chinese revised wechsler adult intelligence scale (WAIS-RC) was administered to all subjects to assess individual intelligence, since a factor analytic study showed that the Wechsler full-scale intelligence quotient (FSIQ) scores accounted for about 90% of the variance in the general intelligence, or $g$ factor [23]. The subjects were divided into two groups on the basis of the individual intelligence quotient score. Thus, the superior intelligence group ($FSIQ > 120$) consisted of 15 women and 17 men (mean age $= 25$, $SD = 3$; mean $FSIQ = 130$, $SD = 5$), while the average intelligence group ($120 > FSIQ > 90$) consisted of 15 women and 12 men (mean age $= 24$, $SD = 4$; mean $FSIQ = 106$, $SD = 8$). There was not a significant difference in age between the two groups. All subjects were recruited by advertisement and gave written informed consent. This study was approved by the ethical committee of Xuanwu Hospital of Capital Medical University.

### B. Imaging Protocol

Magnetic resonance (MR) imaging was acquired using a 3.0-Tesla MR scanner (Magnetom Trio, Siemens, Erlangen, Germany). Functional images were collected axially by using an echo-planar imaging (EPI) sequence sensitive to blood oxygen level-dependent (BOLD) contrast. During the resting state scanning, the subjects were instructed to keep still with their eyes closed, as motionless as possible, and to not to think about anything in particular.

### C. Data Analysis

*1) Preprocessing:* For the present functional magnetic resonance imaging (fMRI) data, several preprocessing steps were used, including 1) correcting for within-scan acquisition time differences between slices; 2) realigning the volumes to the first volume to correct for inter-scan movements; 3) spatially normalizing to a standard EPI template and making a resample; 4) spatially smoothing; 5) linear regression to remove the influence of head motion, whole brain signals, and linear trends; 6) temporally band-pass filtered. Specially, the parameters obtained during movement correction showed that the maximum displacement in the cardinal direction $(x, y, z)$ was not greater than 1 mm, and the maximum spin $(x, y, z)$ was not greater than $1^\circ$ for each participant.

TABLE I
ROI Brain Regions for Default Network

| Brain region | Abbreviations | MNI Coordinates |
|---|---|---|
| Medial prefrontal cortex (anterior) | aMPFC | (-3,54,18) |
| Left superior frontal cortex | L.Sup.F | (-15,54,42) |
| Right superior frontal cortex | R.Sup.F | (18,42,48) |
| Medial prefrontal cortex (ventral) | vMPFC | (-6,36,-9) |
| Left inferior temporal cortex | L.IT | (-60,-9,-24) |
| Right inferior temporal cortex | R.IT | (57,0,-27) |
| Left parahippocampal gyrus | L.PHC | (-24,-18,-27) |
| Right parahippocampal gyrus | R.PHC | (27,-18,-24) |
| Posterior cingulate cortex | PCC | (-3,-48,30) |
| Retrosplenial | Rsp | (9,-54,12) |
| Left lateral parietal cortex | L.LatP | (-48,-69,39) |
| Right lateral parietal cortex | R.LatP | (48,-66,36) |
| Cerebellar tonsils | Cereb | (-6,-54,-48) |

*2) Region Definition:* In the present study, we used *a priori* regions of interest (ROIs) to define the default network as previous studies [24]–[26]. In detail, we defined and extracted the default network using a two-step recursive method. First, we chose an initiating seed within the posterior cingulate cortex (PCC), (MNI coordinates $(0, -54, 27)$) according to the previous study [27] and computed the functional connectivity map for each subject with the initiating seed. Based on the pattern of functional connectivity map of all subjects, we extracted the peak coordinates corresponding to the bilateral Parahippocampal gyrus (PHC) and other regions within the default network, including medial prefrontal cortex and lateral parietal cortex. Since the initiating PCC seed might be not well suitable for the present dataset, we used the peak coordinate within the left PHC obtained in the above analysis to compute the functional connectivity map of the left PHC for all subjects, and then combined the information of the local peak functional correlation to the left PHC along with the *a priori* anatomic knowledge to redefine the coordinates of the PCC and the retrosplenial cortex (Rsp).

Thus, using the above two-step procedure, the following coordinates of *a priori* ROIs were obtained as shown in Table I. Finally, all of ROIs were defined as a spherical region with a radius of 6 mm at the center of the obtained coordinates of *a priori* ROI. Since the size of voxel in the present study was $3 \times 3 \times 3$ mm, each ROI was comprised of 33 voxels.

*3) Individual Functional Connectivity Graph:* After extracting the 13 ROIs for each subject, we computed the functional connectivity between each pair of the 13 ROIs. The functional connectivity was produced by averaging the BOLD time series separately in the two regions, and then computing the Pearson's correlation coefficient between the two averaged time series. The resulting correlation was then transformed to approximate Gaussian distribution using Fisher's r-to-z transformation $z = (1/2)\ln((1+r)/(1-r))$[28]. Thus, for each subject, we obtained a $13 \times 13$ matrix, with each element representing the strength of functional connectivity between the corresponding two brain regions within the default network. Specifically, the diagonal element was self-correlation of the corresponding region. For computational convenience, we set

all the diagonal elements' z value to 2, whose approximate correlation was 0.964.

Although it is not very clear how the brain areas within the default network combine with each other, researchers have found that the functional connectivities within the default network were consistent and replicable in a normal population [1], [3], [29]. In the present study, using the one-sample $t$-test, we found that all functional connectivities within the default network were significantly greater than 0 ($P < 0.05$, FDR corrected). This suggested that the functional connectivity between any two nodes within the default network is positive, which was consistent with previous studies [30], [31]. In addition, although we found that some of the functional connectivity in some subjects was negative, the negative functional connectivity accounted for less than 5% of the number of all the functional connectivity. To adopt the commonly used network measures to investigate the topological characteristics of the default network, we set the negative functional connectivity as 0. This allowed us to use the undirected weighted graph to model the default network. That is, the node of graph was used to denote the brain region within the default network, and the weight of the edge between two nodes was represented to the z-valued strength of functional connectivity between the corresponding two brain regions. Thus, we constructed a complete undirected weighted graph to model the topology of the default network for each subject.

*4) Median Functional Connectivity Graph:* First, we intuitively investigated the average topology of the default network within each of the two groups. For more robustness, we used the median, rather than the mean, of z-valued strength of each functional connectivity to represent the average strength of the functional connectivity. Thus, we obtained a median functional connectivity graph separately for each group, and then analyzed the network measures and topological architecture for the median functional connectivity graph of each group.

In graph theory, the degree $s_i$ of a node $i$ was the number of edges linking to the node, and was defined as [32]

$$s_i = \sum_j w_{ij} \tag{1}$$

where $w_{ij}$ denoted to the weighted edge that connected node $i$ with node $j$, that is, in the present study, the z-valued strength of the functional connectivity between brain region $i$ and brain region $j$. The degree $s_i$ can be used to qualify the extent to which the node was central in the graph. With the node degree, we can define the hub node, which is the node with high degree in a graph.

Here, we calculated the degree for every node of the median functional connectivity graph separately for the two groups. In addition, to graphically represent the architecture of the graph, we used Kamada–Kawai algorithm (fix the first and last nodes) that was implemented in *Pajek* [33]. The Kamada–Kawai algorithm was a force directed graph layout algorithm. The basic idea of this algorithm was to minimize the energy function of the graph by moving the nodes and changing the distance between them. So, the layout of the graph could be used to represent how close the nodes in graph were. Specifically, the layout of the graph was not unique and changeable when using the Kamada–Kawai algorithm. However, in the present study, we noted that two features of the layout were stable. One was the central position of PCC in the layout of default network, whereas another was the segregation of the bilateral PHC and cerebellar tonsils from the other nodes within the default network. Here, we called the nodes except the bilateral PHC and cerebellar tonsils as major nodes within the default network. Accordingly, we made two hypotheses that, 1) PCC was the most important hub node in the default network; 2) the bilateral PHC and cerebellar tonsils were topologically separations from major nodes within the default network. For the first hypothesis, we used the paired test to validate whether PCC was the node with the greatest degree in each subject. For the second one, we still used the paired test to validate whether the average of the shortest path lengths between bilateral PHC (or cerebellar tonsils) and each of the major nodes was significantly greater than the one between any pair of major nodes in each subject.

*5) Comparison of Topological Properties of Graph Between Two Groups:* Next, we used the two-sample $t$-test to investigate whether there was significant difference in some network measures of the graph of the default network between the superior intelligence group and the average intelligence group. These measures included the strength of functional connectivity between any two nodes, node degree of every node, clustering coefficient of every node, the shortest path length between any pair of nodes, and the global efficiency of graph. The definition and significance of degree have been stated in (1).

The clustering coefficient $C_i$ was a typical property of a node in a graph, and it can be used to quantify how close the neighbors of the node $i$ are. Various definitions for clustering coefficient in the weighted graph have been proposed over years. In present study, since the weighted graph was complete, we used the definition as [34]

$$C_i = \frac{\sum_j \sum_k w_{ij} w_{jk} w_{ki}}{\left(\sum_j w_{ij}\right)^2 - \sum_j {w_{ij}}^2} \tag{2}$$

where $w_{ij}$ denoted to the weighted edge that connected node $i$ to node $j$. Thus, it was easy to know the following equation $C_i \in [0, 1]$.

The shortest path lengths play an important role in the transport and communication within a graph. It refers to the length of the path of minimal length between two nodes and can be used to characterize how well two nodes communicate. In this study, the weight of the edge between two nodes was represented to the z-valued strength of functional connectivity, and we set all the diagonal elements of individual functional connectivity matrix to 2 as the above description. Therefore, we defined the distance between two nodes in the graph by subtracting the z-valued strength of functional connectivity from the constant 2. The more general definition of the distance in this study was as follows

$$d_{ij} = \text{constant} - w_{ij} \tag{3}$$

where $w_{ij}$ was the z-valued strength of the functional connectivity between the brain region $i$ to the brain region $j$. Here,

the constant was 2. Thus, it was clear that the distance was inversely related to the strength of the functional connectivity. Then, we computed the shortest path lengths with the Dijkstra's algorithms [35].

With the shortest path lengths, we can define the so-called global efficiency of the graph as [32], [36]

$$E = \frac{1}{N(N-1)} \sum_{i \neq j} \frac{1}{l_{ij}} \tag{4}$$

where $N$ was the number of nodes in the graph, and $l_{ij}$ was the shortest path length between node $i$ and node $j$. The quantity of the efficiency can be used as an indicator of the traffic capacity of a network. Here, we used the global efficiency to qualify the associations between intelligence differences and the functional integration of the default network.

*6) Correlations of Network Measures to FSIQ Scores Across All Subjects:* We correlated the FSIQ scores with network measures across all subjects. These measures included the strength of the functional connectivity, node degree, clustering coefficient, the shortest path length, and global efficiency.

## III. Results

The median functional connectivity matrix and weighted graph for both groups were shown in Fig. 1. As shown in Fig. 1, the homologous brain regions showed the strong functional connectivity. The PCC showed the greatest degree and was situated in the center of the layout of the default network in both of the two groups. We validated that PCC was the node with the greatest degree in the default network (the paired $t$-test, $P < 0.00025$ for both groups). On the other hand, we found that the bilateral PHC and cerebellar tonsils showed the comparative weak connectivity with major nodes in the default network and thus they were topologically segregations in the layout of the default network. As presented in methods, we used the paired $t$-test to validate the result. We found that, the bilateral PHC and cerebellar tonsils showed greater shortest path lengths to the major nodes of the default network in comparison to the nodes within major nodes (bilateral PHC, $P < 0.0000$ for both groups , cerebellar tonsils, $P < 0.0000$ for both groups).

We compared the network measures of the default network between the superior intelligence group and the average intelligence group. We found that there were significant differences in the strength of some functional connectivities between the two groups as shown in the center subplot in Fig. 2 (the two-sample $t$-test, $P < 0.05$, uncorrected), and we found significant differences in some node's degree, including L.IT, L.Sup.F, vMPFC, L.PHC (the two-sample $t$-test, $P < 0.05$, uncorrected), while there were no significant differences in any clustering coefficient between the two groups. We also found significant differences in the shortest path length between the two groups (the two-sample $t$-test, $P < 0.05$, uncorrected). More importantly, we found that there was the significant difference in the global efficiency of the graph of default network (the two-sample $t$-test, $P < 0.035$, uncorrected).

We correlated the network measures with the FSIQ scores across all subjects, and found that there were no significant correlations between the FSIQ scores and some network measures, including node degree, clustering coefficient, and global efficiency (Correlation $R = 0.24$, $P = 0.072$), while some functional connectivities showed the significant correlations to the FSIQ scores, including PCC-vMPFC, Rsp-vMPFC, Rsp-L.PHC, Rsp-R.PHC and R.IT-L.PHC ($P < 0.05$, uncorrected). These correlation results were also shown in Fig. 2.

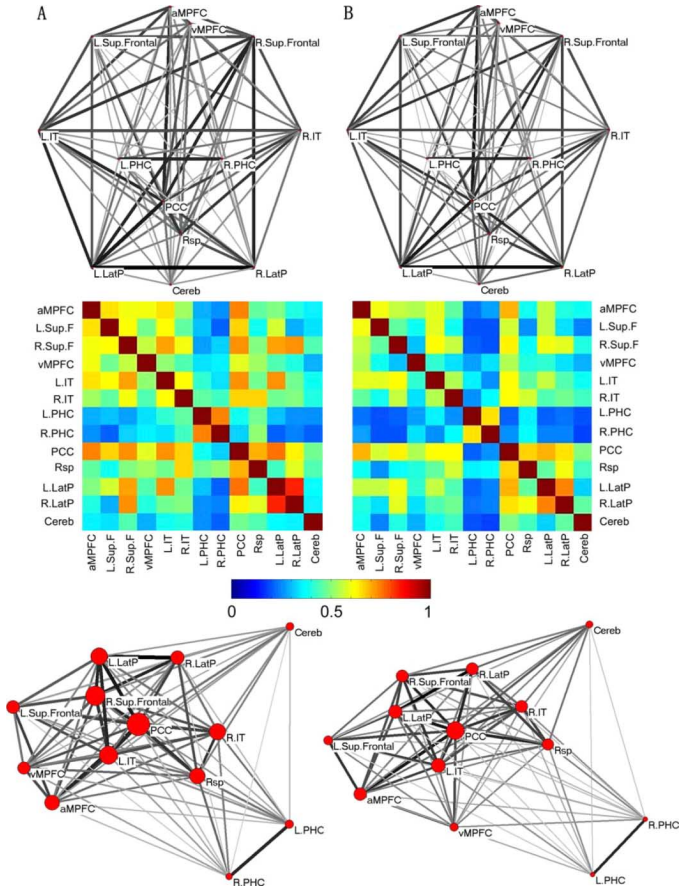


Fig. 1. The median functional connectivity matrix and graph separately for the superior intelligence group (Column A, left) and the average intelligence group (Column B, right). The first row represents the function connectivity between any pair of brain regions in the default network in a pseudoanatomical organization. The gray value of line is proportional to the connection strength. The second row represents the correlation matrices. The third row represents one layout of graph of the default network using the Kamada–Kawai algorithm. The distance between nodes roughly represents how close the brain regions functionally correlated. Node size is proportional to its node degree.

## IV. Discussion

In the study on the default network, researchers can often use PCC as seed region to define and extract the default network [27], [31], [37]. In the present study, using weighted graph theory, we quantitatively confirm that PCC was the most important hub node in the default network, which suggested that PCC could be the center of information processing within the default network. This might be one of the reasons that researchers can use PCC to robustly find the other regions within the default network and further construct the default network.

PCC is located in the posterior part of the cingulate cortex and comprises Brodmann 23, 31. The anatomy of PCC in the macaque monkey has been extensively studied [38]–[40]. Researchers have found that PCC had reciprocal projection with

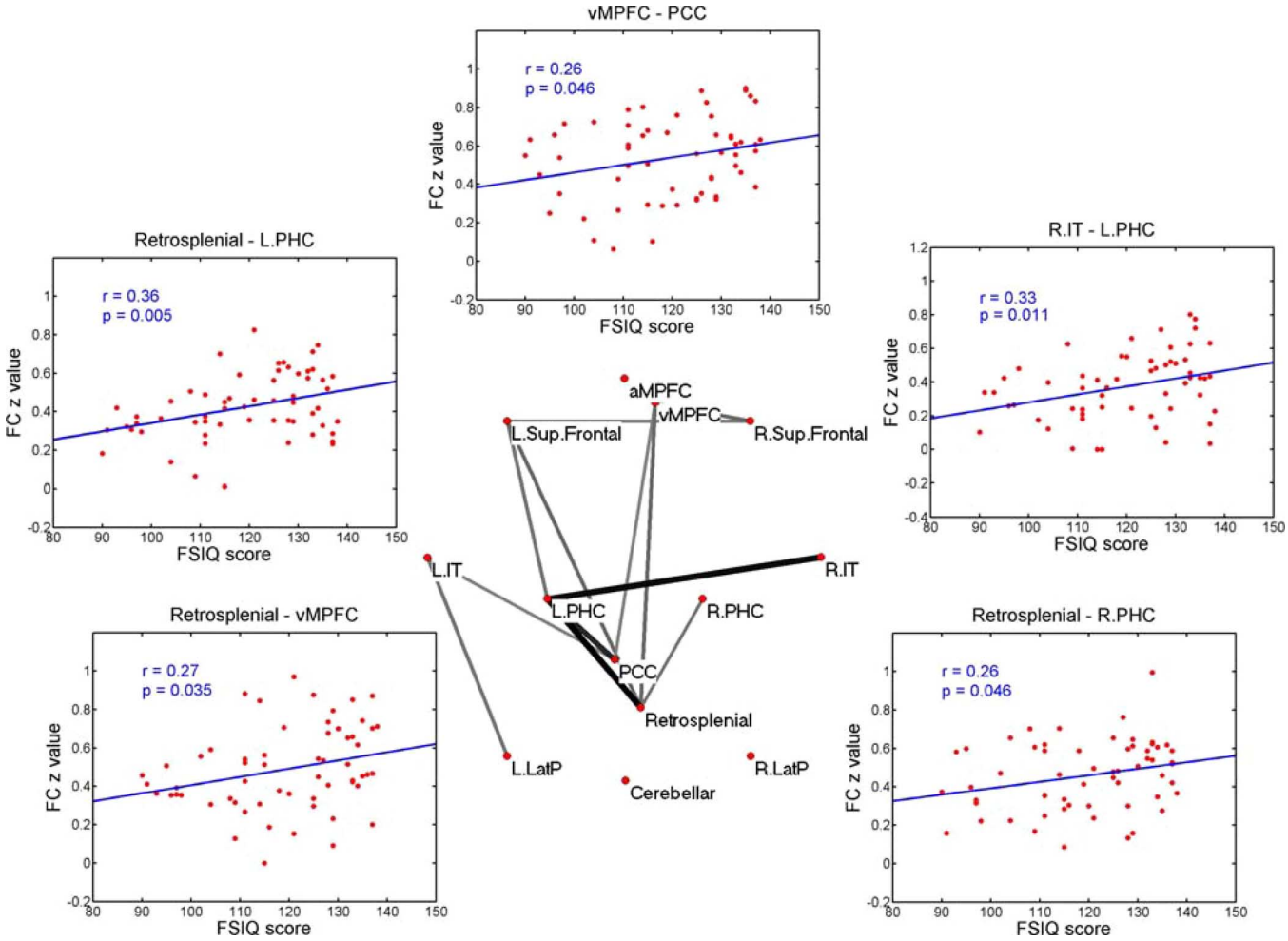


Fig. 2. The significantly different functional connectivity between the superior intelligence group and the average intelligence group and the significant correlations between the strength of the functional connectivity to the FSIQ scores across all subjects. The central subplot shows the significantly different functional connectivity in the strength between the average intelligence group and the superior intelligence group (two-sample $t$-test, $P < 0.05$, uncorrected). The gray value of line in the central subplot is proportion to the score. The significant correlations between the strength of the functional connectivity and the FSIQ scores were shown around the central subplot.

the medial temporal lobes and robust connections with prefrontal cortex and parietal cortex. A study based on human diffusion tensor imaging has found that there were fiber tract connections between PCC and the medial prefrontal cortex [41]. Specially, Hagmann and colleagues mapped white matter cortico–cortical connections with diffusion spectrum imaging and found that the posterior medial regions formed a topologically central core in human brain [42]. Additionally, using the partial correlation analysis method with fMRI data, Fransson and colleagues found that PCC showed strong connections with the rest of brain regions within the default network [43]. The authors suggested that PCC should play a pivotal role in the default network, which was consistent with our present result. In addition, some clinical studies suggested that the abnormality of PCC could be related to some neuropsychiatric diseases. For example, lots of functional studies consistently found that there was significant difference in the activity of PCC between the patients in Alzheimer disease and the normal controls [30], [44], [45]. These evidences from different sources suggested the core importance of PCC within the default network and its significance for human cognitive ability.

At the same time, as the study of default network goes in depth, researchers have recognized that the default network should comprise some interacting subsystems [3]. Among these subsystems, the bilateral Hippocampus (HF) and PHC constitute the medial temporal lobes subsystem (MTLs), which provide information from prior experiences in the forms of memories. The other brain regions within the default network, including the prefrontal cortex and lateral parietal cortex, used the prior information from the MTLs and assimilated what actually happens to adapt and improve the brain's mental capabilities, for example, the anticipatory ability in forms of envisioning future event, self-relevant mental planning, and even mind wandering [1], [3], [46].

Specially, we found that the MTLs showed comparatively greater functional connectivity with Rsp. It suggests that Rsp could play as a transformer in the combination of the MTLs with the other brain regions within the default network. Although it is a posterior part of the cingulate cortex like PCC, Rsp is mainly defined by Brodmann area 29, 26. In animal study, some researchers found that Rsp had dense reciprocal projections with HF and PHC [39], [40]. Grecius and col-

leagues used diffuse tensor imaging to show robust structural connections between the MTLs and Rsp in human brain [41]. On the other hand, researchers found that, relative to the robust posterior midline brain regions and medial prefrontal cortex, the MTLs were less prominent in the task-induced deactivations [3]. Additionally, the functional connectivity of HF showed imperfect overlap with the default network [47]. Fransson and colleagues found weak functional connections between the MTLs and the rest of the brain regions within the default network [43]. In the present study, we found that the MTLs were topologically separations from the other brain regions within the default network. Taking the function of MTLs together, we believe that MTLs play as a retrieving subsystem, analogously as a prior knowledge database, to be involved in the default network.

The neural basis of human intelligence has been investigated for many years. Researchers have found, using various neuroimaging paradigms that have ranged from the structural [48]–[50] to functional imaging [51]–[54], that a brain network characterized by interactions between multiple brain regions supported the intelligence. Specially, in our previous study [17], we found that the strength of the functional connectivity between the brain regions distributed in the frontal, parietal, occipital, and limbic lobes was significantly correlated with individual intelligence scores even in the resting state and in the absence of an explicit cognitive demand. Broadly speaking, there are some pioneering studies to investigate the relationship between the resting state fMRI signals and the individual cognitive performance [15], [16], [18]. Specially, Hampson and colleagues found that the strength of the resting state functional connectivity between PCC and a medial frontal region incorporating portions of the medial frontal gyrus and ventral anterior cingulated cortex were correlated with the subjects' performance in working memory task [15]. Additionally, in another age-related study, Sambataro and colleagues found that the strength of the functional connectivity between PCC and medial prefrontal cortex (MPFC) was positively correlated to the working memory performance [18]. In the present study, we found that some functional connectivities showed the significant positive correlations to the FSIQ scores, including PCC-vMPFC. These results would together suggest the important role of the functional interacting between PCC and MPFC in the cognitive performance. In addition, although we did not find significant positive correlation between the global efficiency of the default network and the FSIQ scores, there were significant differences in the global efficiency between the average intelligence group and the superior intelligence group. As shown in methods, the global efficiency is inversely related to the shortest path length, which roughly means that the global efficiency is related to the strength of functional connectivity in the present study. In comparison to the functional connectivity, the measure of the global efficiency is numerically easier to use to estimate the functional integration of multiple brain regions in a network [36], [55]. In this study, the superior intelligence group showed larger global efficiency of the default network compared to the average intelligence group, which suggests that the subjects with higher intelligence have more integrated functional architecture of the default network.

In this study, we constructed a complete undirected weighted graph to model the topology of default network for each subject. This is significantly different from previous studies. In previous studies, the threshold was applied to produce a binary adjacency matrix or undirected "0–1" graph, irrespective of the strength of the connection between two nodes [24], [26], [56], [57]. Since the functional connectivity between the brain regions within the default network is significantly positive in a normal population, it is difficult to apply a threshold to model the default network as a binary graph. In the present study, we used the z-valued strength of functional connectivity as the weight to model the connection between the brain regions within the default network, which can resolve the issue of threshold in a sense. Unfortunately, we have faced some trouble in the methods, especially in the definition of the weight and the distance. First, although the one-sample $t$-test showed that all of the functional connectivity within the default network was significantly positive in our dataset, we found that some functional connectivities in some subjects were negative. These negative functional connectivities might result from the error in the extraction of ROIs or the registration to the template. Besides, we speculated that the functional separation within the default network might result in the negative functional connectivity in some sense. To adopt the commonly used network measures, such as node degree, global efficiency, and so on, to investigate the topological characteristics of the default network, we set the negative functional connectivity to 0. Although the number of the negative functional connectivity was less than 5% of the number of all the functional connectivity, and we checked and found that there was no significant difference for most of network characteristics in the present study no matter when setting the negative functional connectivity to 0 or not, we remind the reader that there are some limitations to set the negative functional connectivity to 0. Second, we adopted a linear method to define the distance between the nodes as shown in (3). In fact, there are other definitions that can be used as the distance, for example, using the multiplicative inverse of the strength of the functional connectivity as the distance as in [58]. We compared the difference in the shortest path lengths between the two groups when separately using the present subtraction and the multiplicative inverse as the distance. We found that there was significant difference when using different methods to define distance and, it was difficult to explain the results when using the multiplicative inverse as the distance. Since the negative functional connectivity was set to 0, its multiplicative inverse is infinite. Additionally, since the distance defined as (3) is inversely related to the strength of functional connectivity, the difference in the shortest path length between the two groups and the correlations between the shortest path length and the FSIQ scores were both independent on the constant. So we prefer to use the present linear method to define the distance. However, the choice of the constant would influence the significance of difference in global efficiency between the two groups. Thus, it is required to pay much attention to the above two limitations. Future efforts should be made to resolve these issues.

Specially, we chose the left PHC, a region that is subsequently verified to be the topological isolation to the major nodes of the default mode network, as the seed region for defining PCC and

Rsp. Here, our motivation is to use the peak functional correlation between the central nodes, (i.e., PCC and Rsp), and the PHC to verify the functionally separations within the default network. We verified the robustness of the functional connectivity between the other major nodes of the default network, including aMPFC and vMPFC, and the seed regions of PCC and Rsp. So, we believed that the locations of the seed regions of the PCC and Rsp were suitable for the present dataset.

Interestingly, we noted that some artificial cognitive architecture, for example, Adaptive control of thought-rational (ACT-R)[59] and global workspace dynamical architecture [60], had designed some modules or mechanisms to rehearse imaginary events or scenarios, and then use the information from the rehearsal to modulate the actual behavior. The architectures suggest the importance of the ability to reflect on the past and predict the future [61], which are similar to the cognitive functions of the default network in the human brain. Specially, there are some arguments about the extension of the physiological significance of the default network, so more efforts are required to make sense of the default network, especially its functions and organization structure. We believe that the ongoing studies on the intrinsic activity of the human brain will bring more cues, not only for human cognitive functions, but also for the developmental artificial cognitive system. Here, we suggest that the topological pattern of a network comprising specifically functional distributed subsystems and the information hub nodes that converges these subsystems might be important for a developmental artificial intelligent system.

In summary, using the graph theory, we found that PCC showed the greatest degree in comparison to the other brain regions within the default network, which quantitatively suggests that PCC was the hub node for information integration of default network. On the other hand, we found that the bilateral PHC and cerebellar tonsils showed the significantly weaker connectivity with the major nodes in the default network and thus, they were topologically segregations in the layout of the default network. This suggests that MTLs and cerebellar tonsils play as a subsystem to be involved in the default network. More importantly, we found that the strength of some functional connectivities and the global efficiency of the default network were significantly different between the superior intelligence group and the average intelligence group, which indicates that the functional integration of the default network might be related to the individual intelligent performance.

## ACKNOWLEDGMENT

The authors would like to thank the individuals involved in this study and their families. The authors are grateful to two anonymous reviewers, who gave some suggestions that improved the manuscript.

## REFERENCES

[1] M. Raichle, A. MacLeod, A. Snyder, W. Powers, D. Gusnard, and G. Shulman, "A default mode of brain function," *Proc. Nat. Acad. Sci. USA.*, vol. 98, pp. 676–682, Jan. 2001.

[2] M. Raichle and M. Minton, "Brain work and brain imaging," *Annu. Rev. Neurosci.*, vol. 29, pp. 449–476, 2006.

[3] R. Buckner, J. Andrews, and D. Schacter, "The brain's default network," *Annu. Acad. Sci.*, vol. 1124, pp. 1–38, 2008.

[4] M. Raichle, "The brain's dark energe," *Science*, vol. 314, pp. 1249–1250, 2006.

[5] M. Raichle and A. Snyder, "A default mode of brain function: A brief history of an evolving idea," *Neuroimage*, vol. 37, pp. 1083–1090, 2007.

[6] R. Buckner and J. Vincent, "Unrest at rest: Default activity and spontaneous network correlations," *Neuroimage*, vol. 37, pp. 1091–1096, 2007.

[7] A. Morcom and P. Fletcher, "Does the brain have a baseline? Why we should be resisting a rest," *Neuroimage*, vol. 37, pp. 1073–1082, 2007.

[8] M. D. Greicius, G. Srivastava, A. L. Reiss, and V. Menon, "Default-mode network activity distinguishes alzheimer's disease from healthy aging: Evidence from functional mri," *Proc. Nat. Acad. Sci. USA*, vol. 101, pp. 4637–4642, Mar. 2004.

[9] Y. Zhou, M. Liang, L. Tian, K. Wang, H. Liu, Y. Hao, Z. Liu, and T. Jiang, "Functional disintegration in paranoid schizophrenia using resting-state fmri," *Schizophrenia Res.*, vol. 97, pp. 194–205, 2007.

[10] M. Boly, A. Vanhaudenhuyse, L. Tshibanda, M. A. Bruno, P. Boveroux, Q. Noirhomme, C. Schnakers, A. Demertzi, D. Ledoux, B. Lambermont, G. Moonen, R. Dondelinger, C. Phillips, P. Maquet, and S. Laureys, "Default network resting state connectivity integrity reflects the level of consciousness impairment in brain-injured patients. An fmri study in brain death, coma, vegetative state, minimally conscious state, and locked-in syndrome," in *Proc. 18th Meeting Eur. Neurolog. Soc.*, Nice, France, 2008, p. 179.

[11] R. Jung and R. Haier, "The parieto-frontal integration theory (p-fit) of intelligence: Converging neuroimaging evidence," *Behav. Brain Sciences*, vol. 30, pp. 135–154, 2007.

[12] J. R. Gray and P. M. Thompson, "Neurobiology of intelligence: Science and ethics," *Nature Rev. Neurosci.*, vol. 5, pp. 471–482, 2004.

[13] M. J. Boivin, B. Giordani, S. Berent, D. A. Amato, S. Lehtinen, R. A. Koeppe, H. A. Buchtel, N. L. Foster, and D. E. Kuhl, "Verbal fluency and positron emission tomographic mapping of regional cerebral glucose metabolism," *Cortex*, vol. 28, pp. 231–239, 1992.

[14] R. Haier, "Individual differences in general intelligence correlate with brain function during nonreasoning tasks," *Intelligence*, vol. 31, pp. 429–441, 2003.

[15] M. Hampson, N. R. Driesen, P. Skudlarski, J. C. Gore, and R. T. Constable, "Brain connectivity related to working memory performance," *J. Neurosci.*, vol. 26, p. 13338, 2006.

[16] W. Seeley, V. Menon, A. Schatzberg, J. Keller, G. Glover, H. Kenna, A. Reiss, and M. Greicius, "Dissociable intrinsic connectivity networks for salience processing and executive control," *J. Neurosci.*, vol. 27, pp. 2349–2356, Feb. 2007.

[17] M. Song, Y. Zhou, J. Li, Y. Liu, L. Tian, C. Yu, and T. Jiang, "Brain spontaneous functional connectivity and intelligence," *Neuroimage*, vol. 41, pp. 1168–1176, Jul. 2008.

[18] F. Sambataro, V. P. Murty, J. H. Callicott, H.-Y. Tan, S. Das, D. R. Weinberger, and V. S. Mattay, "age-related alterations in default mode network: Impact on working memory performance," *Neurobiol. Aging*, to be published.

[19] D. H. Ingvar, *Memory of the Future: An Essay on the Temporal Organization of Conscious Awareness*. New York: Springer, 1985, vol. 4, pp. 127–136.

[20] D. Amodio and C. Frith, "Meeting of minds: The medial frontal cortex and social cognition," *Nature Rev. Neurosci.*, vol. 7, pp. 268–277, Apr. 2006.

[21] J. Hawkins, *On Intelligence*. New York: Owl Books, 2005.

[22] D. T. Gilbert, *Stumbling on Happiness*. New York: Knopf, 2006.

[23] A. R. Jensen, *Bias in Mental Testing*. New York: Free Press, 1980.

[24] D. A. Fair, N. U. F. Dosenbach, J. A. Church, A. L. Cohen, S. Brahmbhatt, F. M. Miezin, D. M. Barch, M. E. Raichle, S. E. Petersen, and B. L. Schlaggar, "Development of distinct control networks through segregation and integration," *Proc. Nat. Acad. Sci. USA*, vol. 104, pp. 13 507–13 512, Aug. 2007.

[25] N. U. F. Dosenbach, D. A. Fair, F. M. Miezin, A. L. Cohen, K. K. Wenger, R. A. T. Dosenbach, M. D. Fox, A. Z. Snyder, J. L. Vincent, M. E. Raichle, B. L. Schlaggar, and S. E. Petersen, "Distinct brain networks for adaptive and stable task control in humans," *Proc. Nat. Acad. Sci. USA*, vol. 104, pp. 11 073–11 078, Jun. 2007.

[26] D. Fair, A. Cohen, N. Dosenbach, J. Church, F. Miezin, D. Barch, M. Raichle, S. Petersen, and B. Schlaggar, "The maturing architecture of the brain's default network," *Proc. Nat. Acad. Sci. USA*, vol. 105, pp. 4028–4032, Mar. 2008.

[27] J. R. Andrews-Hanna, A. Z. Snyder, J. L. Vincent, C. Lustig, D. Head, M. E. Raichle, and R. L. Buckner, "Disruption of large-scale brain systems in advanced aging," *Neuron*, vol. 56, pp. 924–935, 2007.

[28] W. H. Press, *Numerical Recipes in C*. Cambridge, U.K.: Cambridge University Press, 1992.
[29] B. J. Harrison, J. Pujol, M. Lopez-Sola, R. Hernandez-Ribas, J. Deus, H. Ortiz, C. Soriano-Mas, M. Yucel, C. Pantelis, and N. Cardoner, "Consistency and functional specialization in the default mode brain network," *Proc. Nat. Acad. Sci. USA*, vol. 105, pp. 9781–9786, Jul. 2008.
[30] M. D. Greicius, B. Krasnow, A. L. Reiss, and V. Menon, "Functional connectivity in the resting brain: A network analysis of the default mode hypothesis," *Proc. Nat. Acad. Sci. USA*, vol. 100, pp. 253–258, Jan. 2003.
[31] M. D. Fox, A. Z. Snyder, J. L. Vincent, M. Corbetta, D. C. V. Essen, and M. E. Raichle, "The human brain is intrinsically organized into dynamic, anticorrelated functional networks," *Proc. Nat. Acad. Sci. USA*, vol. 102, pp. 9673–9678, Jul. 2005.
[32] S. Boccaletti, V. Latora, Y. Moreno, M. Chavez, and D. Hwang, "Complex networks: Structure and dynamics," *Phys. Rep.-Rev. Section Phys. Lett.*, vol. 424, pp. 175–308, Feb. 2006.
[33] V. Batagelj and A. Mrvar, "Pajek – Analysis and visualization of large networks," in *Proc. 9th Int. Symp. Graph Drawing*, Vienna, Austria, 2001, pp. 477–478.
[34] B. Zhang and S. Horvath, "A general framework for weighted gene co-expression network analysis," *Stat. Appl. Genetics Molecular Biol.*, vol. 4, p. 17, 2005.
[35] E. W. Dijkstra, "A note on two problems in connection with graphs," *Numerische Math*, vol. 1, pp. 269–271, 1959.
[36] S. Achard and E. Bullmore, "Efficiency and cost of economical brain functional networks," *PLoS Comput. Bio.*, vol. 3, p. e17, Feb. 2007.
[37] J. L. Vincent, G. H. Patel, M. D. Fox, A. Z. Snyder, J. T. Baker, D. C. V. Essen, J. M. Zempel, M. C. L. H. Snyder, and M. E. Raichle, "Intrinsic functional architecture in the anaesthetized monkey brain," *Nature*, vol. 447, pp. 83–86, May 2007.
[38] Y. Kobayashi and D. G. Amaral, "Macaque monkey retrosplenial cortex: I. Three-dimensional and cytoarchitectonic organization," *J. Compar. Neurol.*, vol. 426, pp. 339–365, Oct. 2000.
[39] Y. Kobayashi and D. G. Amaral, "Macaque monkey retrosplenial cortex:II. Cortical afferents," *J. Compar. Neurol.*, vol. 466, pp. 48–79, Nov. 2003.
[40] Y. Kobayashi and D. G. Amaral, "Macaque monkey retrosplenial cortex: III. Cortical afferents," *J. Compar. Neurol.*, vol. 502, pp. 810–833, Jul. 2007.
[41] M. D. Greicius, V. M. K. Supekar, and R. E. Dougherty, "Resting-state functional connectivity reflects structural connectivity in the default mode network," *Cereb. Cortex*, vol. 19, pp. 72–78, Apr. 2009.
[42] P. Hagmann, L. Cammoun, X. Gigandet, R. Meuli, C. J. Honey, V. Wedeen, and O. Sporns, "Mapping the structural core of human cerebral cortex," *PLoS Biol.*, vol. 6, pp. 1479–1493, Jul. 2008.
[43] P. Fransson and G. Marrelec, "The precuneus/posterior cingulate cortex plays a pivotal role in the default mode network: Evidence from a partial correlation network analysis," *Neuroimage*, vol. 42, pp. 1178–1184, Sep. 2008.
[44] Y. He, L. Wang, Y. Zang, L. Tian, X. Zhang, K. Li, and T. Jiang, "Regional coherence changes in the early stages of alzheimer's disease: A combined structural and resting-state functional MRI study," *Neuroimage*, vol. 35, pp. 488–500, Apr. 2007.
[45] G. W. Small, S. Y. Bookheimer, P. M. Thompson, G. M. Cole, S. C. Huang, V. Kepe, and J. R. Barrio, "Current and future uses of neuroimaging for cognitively impaired patients," *Lancet Neurol.*, vol. 7, pp. 161–172, Feb. 2008.
[46] M. F. Mason, M. I. Norton, J. D. V. Horn, D. M. Wegner, S. T. Grafton, and C. N. Macrae, "Wandering minds: The default network and stimulus-independent thought," *Science*, vol. 315, pp. 393–395, Jan. 2007.
[47] J. L. Vincent, A. Z. Snyder, M. D. Fox, B. J. Shannon, J. R. Andrews, M. E. Raichle, and R. L. Buckner, "Coherent spontaneous activity identifies a hippocampal-parietal memory network," *J. Neurophysiol.*, vol. 96, pp. 3517–3531, Dec. 2006.
[48] R. J. Haier, R. E. Jung, R. A. Yeo, K. Head, and M. T. Alkire, "Structural brain variation and general intelligence," *Neuroimage*, vol. 23, pp. 425–433, 2004.
[49] P. Shaw, D. Greenstein, J. Lerch, L. Clasen, R. Lenroot, N. Gogtay, A. Evans, J. Rapoport, and J. Giedd, "Intellectual ability and cortical development in children and adolescents," *Nature*, vol. 440, pp. 676–679, 2006.
[50] R. Colom, R. E. Jung, and R. J. Haier, "Distributed brain sites for the g-factor of intelligence," *Neuroimage*, vol. 31, pp. 1359–1365, 2006.
[51] G. Esposito, B. S. Kirkby, J. D. V. Horn, T. M. Ellmore, and K. F. Berman, "Context-dependent, neural system-specific neurophysiological concomitants of ageing: Mapping pet correlates during cognitive activation," *Brain*, vol. 122, pp. 963–979, 1999.
[52] J. R. Gray, C. F. Chabris, and T. S. Braver, "Neural mechanisms of general fluid intelligence," *Nature Neurosci.*, vol. 6, pp. 316–322, 2003.
[53] T. Fangmeier, M. Knauff, C. C. Ruff, and V. Sloutsky, "Fmri evidence for a three-stage model of deductive reasoning," *J. Cogn. Neurosci.*, vol. 18, pp. 320–334, 2006.
[54] K. H. Lee, Y. Y. Choi, J. R. Gray, S. H. Cho, J. H. Chae, S. Lee, and K. Kim, "Neural correlates of superior intelligence: Stronger recruitment of posterior parietal cortex," *Neuroimage*, vol. 29, pp. 578–586, 2006.
[55] E. Bullmore and O. Sporns, "Complex brain networks: Graph theoretical analysis of structural and functional systems," *Nature Rev. Neurosci.*, vol. 10, pp. 186–198, 2009.
[56] Y. Liu, M. Liang, Y. Zhou, Y. He, Y. H. Hao, M. Song, C. S. Yu, H. H. Liu, Z. N. Liu, and T. Z. Jiang, "Disrupted small-world networks in schizophrenia," *Brain*, vol. 131, pp. 945–961, 2008.
[57] C. J. Stam, B. F. Jones, G. Nolte, M. Breakspear, and P. Scheltens, "Small-world networks and functional connectivity in alzheimer's disease," *Cereb. Cortex*, vol. 17, pp. 92–99, 2007.
[58] Y. Iturria-Medina, R. Sotero, E. Canales-Rodríguez, Y. Alemán-Gómez, and L. Melie-García, "Studying the human brain anatomical network via diffusion-weighted mri and graph theory," *Neuroimage*, vol. 40, pp. 1064–1076, 2008.
[59] J. Anderson, D. Bothell, M. Byrne, S. Douglass, C. Lebiere, and Y. Qin, "An integrated theory of the mind," *Psychol. Rev.*, vol. 111, pp. 1036–1060, Oct. 2004.
[60] M. Shanahan, "A cognitive architecture that combines internal simulation with a global workspace," *Consciousness Cogn.*, vol. 15, pp. 443–449, 2006.
[61] D. Vernon, G. Metta, and G. Sandini, "A survey of artificial cognitive systems: Implications for the autonomous development of mental capabilities in computational agents," *IEEE Trans. Evol. Comput.*, vol. 11, pp. 151–180, Apr. 2007.

**Ming Song** (M'09) received the Ph.D. degree from the Institute of Automation, the Chinese Academy of Sciences, Beijing, China, in 2008.

He is currently an Assistant Professor at the Chinese Academy of Sciences. His research interests include the analysis of functional magnetic resonance imaging and brain computer interface.

**Yong Liu** has been an Assistant Professor with the Institute of Automation, the Chinese Academy of Sciences, Beijing, China, since 2008. His work focuses on the brain network analysis with functional magnetic resonance imaging and its application in cognitive disorders.

**Yuan Zhou** received the Ph.D. degree from the Institute of Automation, the Chinese Academy of Sciences, Beijing, China, in 2007.

She currently works as an Assistant Professor at the Institute of Psychology, the Chinese Academy of Sciences. Her research interests include functional neuroimaging of psychiatry and neural basis of decision making.

**Kun Wang** received the Ph.D. degree from the Institute of Automation, the Chinese Academy of Sciences, Beijing, China, in 2009.

He is currently working at the General Electric Company in Beijing.

**Chunshui Yu** worked in the Department of Radiology, Xuanwu Hospital of Capital Medical University, Beijing, China. He is currently working at Tianjin Medical University General Hospital.

**Tianzi Jiang** (M'98–SM'04) received the B.Sc. degree in scientific computing from Lanzhou University, Lanzhou, China, in 1984, and the M.Sc. degree in applied mathematics and Ph.D. degree in scientific computing from Zhejiang University, Hangzhou, China, in 1992 and 1994, respectively.

From 1984 to 1989, he was an Associate Lecturer at Suzhou Silk Engineering Institute. From 1994 to 1996, he worked as a Postdoctoral Research Fellow, and from 1996 to 1999, as an Associate Professor at the National Laboratory of Pattern Recognition (NLPR), Chinese Academy of Sciences. From 1997 to 1999, he was a Vice-Chancellor's Postdoctoral Research Fellow at the University of New South Wales, Australia, while adjunctively with NLPR. From 1999 to 2000, he was a Visiting Scientist at the Max-Planck Institute of Cognitive Neuroscience, Leipzig, Germany. From 2000 to 2001, he was a Research Fellow at the Queen's University of Belfast, U.K. Since 2001, he has been a Full Professor and the Director of Medical Imaging and Computing Group at the NLPR, supported by the Hundred Talents Programs of the Chinese Academy of Sciences. He has also been the Deputy Director of the NLPR from 2003 to 2006 and the Chinese Director of the Sino-French Laboratory in Computer Science, Automation, and Applied Mathematics (LIAMA) since 2006. His research interests include anatomical and functional brain imaging, medical image analysis, complex brain networks, imaging genetics, and applied mathematics. He is the author or coauthor of over 130 reviewed journal papers in these fields and the coeditor of three issues of the Lecture Notes in Computer Sciences.

Dr. Jiang is an Associate Editor of the IEEE TRANSACTIONS ON MEDICAL IMAGING, the IEEE TRANSACTIONS ON AUTONOMOUS MENTAL DEVELOPMENT, and a member of the editorial boards of *Neuroimage*, as well as five other journals. He serves as the Executive General Chair of the Second International Workshop on Medical Imaging and Augmented Reality (MIAR'04), the Program Co-Chair of the Third International Workshop on Medical Imaging and Augmented Reality (MIAR'06), and the General Chair of Medical Image Computing and Computer Assisted Intervention 2010 (MICCAI'2010). He is a member of the scientific committees of a number of international conferences in medical imaging and related fields. He was awarded the National Distinguished Youth Foundations Award by Chinese Government in 2004, the Natural Science Award of China in 2004, and the Natural Science Award of the Chinese Academy of Sciences in 1996.